Velocity smoothing before depth migration: Does it help or hurt?

Ken Larner and Carlos Pacheco
Center for Wave Phenomena, Colorado School of Mines, Golden, CO 80401

ABSTRACT
Previous studies of the sensitivity of depth migration to smoothing of the migration-velocity model have treated smoothing of an initially correct model. Aside from the relatively small amount of smoothing that is needed for imaging with Kirchhoff migration and that does no harm to imaging with finite-difference migration, smoothing of the model changes the model from the true one, so those studies have shown the less smoothing the better. Because we never know the subsurface velocity function with perfect accuracy, imaging is always compromised to some extent by error in the migration-velocity model. Given that reality, perhaps some amount of smoothing of the inevitably erroneous velocity model could improve quality of the migrated image.
We have performed a number of tests of imaging with erroneous velocity models for a simple synthetic 2D model of reflectors beneath salt. The salt layer has a chirp-shape boundary so that we could assess imaging quality as a function of lateral wavelength of velocity variation in the overburden. Errors that we introduce into the velocity model include lateral and vertical shifting of the chirp-shape (usually top-of-salt) boundary, and erroneous amplitude of the chirp, including random errors in the chirp shape. Primarily with poststack migration of modeled exploding-reflector, we assess sub-salt image quality for migrations with many different smoothings of erroneous velocity models. We find that, depending on the type and size of error in the shape of the top-of-salt boundary, as well as the lateral wavelength of the chirp, smoothing of the erroneous velocity model before migration can benefit image quality, sometimes substantially. The form of error that can most benefit from smoothing is error in the shape, as opposed to position, of the salt boundary. This observation, based on numerous tests with exploding-reflector data, is supported by a small number of tests with smoothing of the erroneous velocity model in prestack migration.

Key words: velocity smoothing, depth migration

1 INTRODUCTION

No factor is of larger importance to imaging quality in depth migration than accuracy of the velocity model used for the migration. Velocity information, however, is inevitably erroneous to some extent. Finding sufficiently accurate velocity for migration is an especially difficult task in complex regions such as beneath salt in the Gulf of Mexico, an impediment to efficient exploration and development there (Paffenholz, 2001).

Because information about the spatial variation of subsurface velocity can never be known in detail, in practice estimated velocities are routinely smoothed over space prior to using them for migration. Moreover, because Kirchhoff-type migration algorithms obtain their traveltime information from some form of ray tracing, the velocities used must be spatially smoothed to insure stability in the ray computations.

Any smoothing changes the subsurface velocity model and hence the migration result, so too much smoothing will certainly lead to distortion in migrated images. Of importance, then, is to know how much smoothing of the migration velocity field becomes too much.

Various studies, notably those of Versteeg (1993), Gray (2000), and Paffenholz et al. (2001), have aimed at providing guidance on the appropriate amount of spatial smoothing of velocity for depth migration. A common conclusion of those studies, all of which involved smoothing of known velocities in complex two-dimensional (2D) synthetic datasets such as the Marmousi, Sigsbee2, and SEG-EAGE salt models, is that the appropriate amount of smoothing is both model- and depth-dependent. The study of Gray (2000), which focused on Kirchhoff migration, found that, although some smoothing is necessary for that approach, "too little smoothing produced a better image than too much smoothing" because too much smoothing will change the velocity model substantially, perhaps to the extent of removing geologic plausibility.

Because Versteeg (1993) did his migrations with a wavefield-migration approach, which had no dependence on ray tracing, smoothing of the velocity was not essential to overcome a deficiency of the migration method. Paralleling a conclusion of Jannane et el. (1989), Versteeg argued that the velocity model need not include spatial wavelengths smaller than an amount governed by the wavelengths for frequencies in the data, with further dependence on the complexity of the velocity model. His tests showed that smoothing of the known velocity model up to a certain amount (about 200 m for realistic frequencies in the Marmousi data set) was quite acceptable.

In their migration tests with the Sigsbee2 model, Paffenholz et al. (2001) demonstrated the clear superiority of wavefield migration (e.g., finite-difference migration) over Kirchhoff migration when the migration velocity model is known perfectly, but "the advantage of wavefield migration disappears if the (salt) velocity contains errors." They also showed degradation in sub-salt imaging when the migration-velocity model used is erroneous, either because of error in the shape of the salt or because smoothing of the correct model is too large to some extent.

In all of the studies mentioned above, the tests with smoothing for migration involved smoothing of the known, true velocity model. Recall, however, that one of the reasons for smoothing is that we cannot know the true velocity structure in detail – and sometimes we have rather poor information about the velocity structure. It therefore is appropriate to conduct studies in which the smoothing is applied not to the known, correct velocity model but to models that are erroneous. Then, depending on complexity of the velocity model, amount of error in that model, depth of target beneath the erroneous overburden, and frequency content in the data, some degree of smoothing is likely optimal in the sense of yielding a better image of the target than is use of either less or more smoothing.

In the study here, we perform migrations with smoothed versions of erroneous velocity models and make a start at answering the question "does smoothing of the erroneous velocity field help or hurt the quality of the migrated result?"

As in the references mentioned above, our tests make use of synthetic data. Most of our models, however, are much more simple than those in the published studies, with little attempt to mimic realistic subsurface structure. We introduce errors in the shape of the modeled salt and migrate the data when different degrees of spatial smoothing are applied to the erroneous velocity models.

In order to perform enough tests to draw general conclusions here, most of tests entail 2D modeling and migration. Moreover, for reasons discussed below, most involve poststack migrations of data generated under the exploding-reflector assumption.

2 GENERIC MODEL

The simple (we might say simplistic) model, on which we focus most of the tests is exemplified by any of the six models shown in Figure 1. This model, which we call the *generic model*, looks like no salt structure and sub-salt configuration in the real subsurface. It consists of a sub-horizontal, high-velocity 'salt layer', with a chirp-shape for either the top or bottom of salt, beneath a homogeneous layer and above a half-space. That half-space is also homogeneous, except for four sets of embedded reflecting segments, the targets we wish to image. Each set consists of five plane-dipping reflecting segments, with dips ranging from 0 to 40 degrees, in 10-degree increments. One of the upper two sets has reflector dip increasing from left to right, and the other has dip increasing from right to left. This pattern of target reflector dip allows us to assess the relationship between wavelength of lateral velocity variation in the overburden and sub-salt image quality, as well as illumination issues, as they relate to reflector dip. The lower two sets of reflectors have the same form as the upper ones; they are included so that we can observe changes in the quality of imaging with target depth beneath the salt. Use of a chirp shape for the top or bottom of the salt allows systematic analysis of sub-salt image quality as a function of lateral wavelength of salt shape.

Use of such a simple model has its advantages and disadvantages. The model avoids many of the complexities of data from a Marmousi or even Sigsbee2 model, not to mention those in true salt areas. Moreover, use of the chirp shape allows somewhat systematic assessment of modeled sub-salt imaging. The primary disadvantage of the generic model is that it cannot come close to modeling realistic salt shape, let alone the many issues that confound sub-salt imaging.

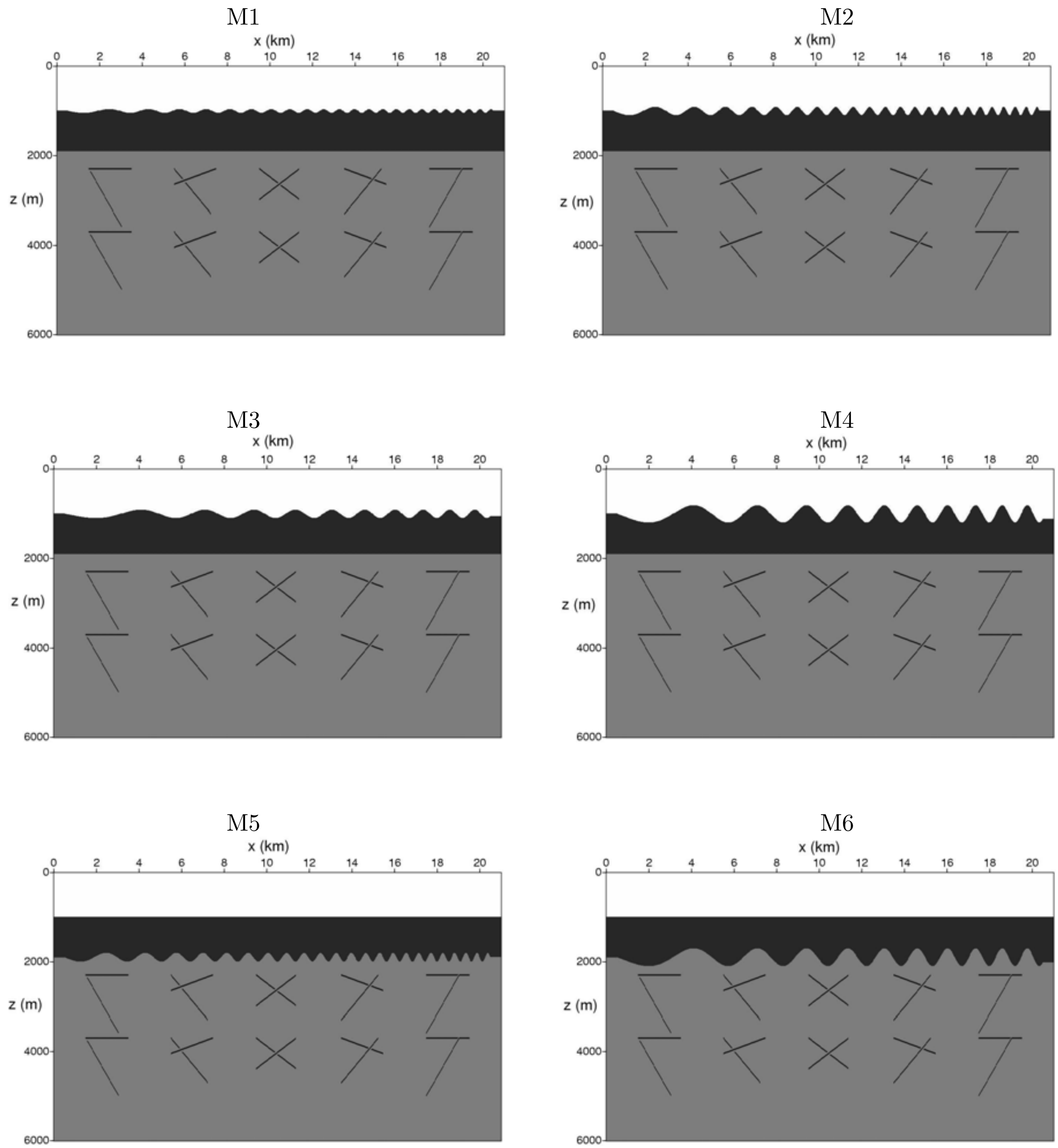

Figure 1. Velocity models M1-M6 used to generate the synthetic data. Lateral position is denoted by x, and depth by z.

Simple as it is, the generic model nevertheless is characterized by enough parameters that comprehensive study of imaging would require a large number of tests of models with many different combinations of values for those parameters. Parameters of the generic model include

- average depth of the top and bottom of the salt
- velocities of the salt and of the layers above and below
- parameters of the chirp-shape top or bottom of salt, specifically
  - amplitude of the chirp
  - range of spatial wavelengths of the chirp
- target depths

Our study can only spottily cover the large combi-

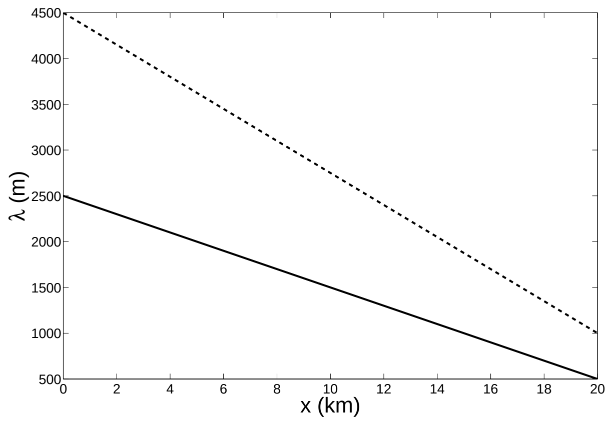

Figure 2. Range of spatial wavelengths for the two chirps used in our study. The solid line shows wavelength λ as a function of lateral position for models M1, M2, and M5; the dashed line shows wavelength for models M3, M4, and M6.

nation of pertinent values for these many parameters. Moreover, none of the six models in Figure 1 exhibits the large structural size of the salt in, for example, the Sigsbee2 model. So, the study is a mere start.

When we consider the different forms of error in the velocity models and differing amounts of smoothing of those erroneous models, the number of tests to perform could further multiply greatly. Errors could arise in all of the parameters (except for the sub-salt reflector description) listed above. For example, the chirp-shape top of salt used for the migration-velocity model could be shifted laterally or vertically from the true position, or have erroneous amplitude.

Our tests with the generic model all involve the six models in Figure 1. All six have velocities of 2000 m/s, 4500 m/s, and 3500 m/s for the top layer, salt layer, and half-space, respectively. For all six models, the average depth of the top and bottom of the salt is 1000 m and 1900 m, respectively. Models M1, M2, and M5 have the same range of spatial wavelength for the chirp, and Models M3, M4, and M6 have a higher range of spatial wavelength. The variation of spatial wavelength with horizontal location is shown in Figure 2. Other differences among the six models are in the amplitude of the chirp shape. Table 1 summarizes the parameter values for the chirp in each model.

Another important parameter for the tests would be the range of frequencies contained in the seismic wavelet used in the wavefield modeling. All of our tests involve just one choice of input wavelet – a Ricker wavelet, with dominant frequency of 15 Hz.

model	λ_{max} (m)	λ_{min} (m)	h (m)	top	bottom
M1	2500	500	50	X	
M2	2500	500	100	X	
M3	4500	1000	100	X	
M4	4500	1000	200	X	
M5	2500	500	50		X
M6	2500	500	100		X

Table 1. Chirp parameters for the generic velocity model used in the study. The parameter h is the ampliitude of the chirp, i.e., the peak departure of salt-boundary depth from its average value.

3 ZERO-OFFSET VERSUS EXPLODING-REFLECTOR DATA

Ultimately one might prefer that a study of the sensitivity of sub-salt imaging to errors in the velocity model be done with 3D prestack depth migration applied to modeled 3D data. The cost of such a study is clearly prohibitive, certainly in this decade. Among the many other complexities of such a study would be the issue of how to define a useful 3D extension of the chirp model.

Our study therefore is strictly limited to 2D. Even 2D prestack depth migration imposes too large a computational cost for other than a small number of token comparison tests with the generic model. In order to do enough comparisons, we limited the study primarily to imaging with poststack migration. The simplification doesn't stop here, however. We can envision three different forms of input to poststack migration: (1) modeled data from many source-to-receiver offsets that have been stacked, (2) zero-offset (ZO) data extracted from normal-moveout-corrected and unstacked modeled data, and (3) exploding-reflector (ER) modeled data. We did tests with all three forms, but the largest number with exploding-reflector data.

The choice of exploding-reflector data may seem puzzling. One reason for this choice is that generation of ER data is least computationally costly. We use a finite-difference code, second-order in time, fourth-order in space, for the modeling; the cost of modeling zero-offset data would be essentially the same as that of modeling a full prestack data set. But there is another reason for choosing exploding-reflector data over extracted zero-offset data.

Seismic data that result from ER modeling are largely equivalent to, but differ in important respects from, either ZO or common-midpoint (CMP) stacked data, particularly in the presence of strong lateral velocity variation (Kjartasson & Rocca, 1979) and (Spetzler & Snieder, 2001). Moreover, the pattern of multiples and the relative amplitudes of the primaries and multiples differ among the three forms of data.

So, why do we consider a study using ER data to be useful? Because poststack migration is based on the exploding-reflector assumption, such migration of zero-offset data would be erroneous even if the migration velocity were correct. In contrast, because poststack (i.e., zero-offset) migration and exploding-reflector modeling of primaries are essentially exact inverses of one another, we can count on accurate migration of ER primaries when we use the correct migration velocities. Therefore, sensitivity of imaging to errors in velocity, including smoothing of erroneous velocity, is best isolated when we apply poststack migration to ER data.

That ER and ZO data differ from one another, as do the results of poststack migration applied to these two forms of data, is exhibited in Figures 3 and 4. The differences between the ER and ZO sections for models M1, M2, and M4, in Figure 3, are striking. Particularly for models with larger chirp amplitude and in regions of the model with smaller chirp wavelength, sub-salt reflections show more numerous triplications characteristic of caustics and multi-pathing in the overburden. The exploding-reflector sections exhibit less loss of amplitude with time and more complete expression of the diffractions than do the zero-offset sections. Since migration aims to collapse diffractions, the distorted and incomplete diffractions in the ZO data will be poorly collapsed in poststack-migrated results. The stronger amplitudes at late time in the ER data result from the weaker geometric spreading from sources that are, in effect, placed on the exploding reflectors than the spreading from the surface line sources for the ZO data. Finally, as expected, the timing and amplitudes of multiples in the exploding-reflector sections differ from those in the counterpart zero-offset sections. The multiples in these data are internal ones. Surface multiples are largely absent because absorbing boundary conditions (Clayton & Engquist, 1977) were used for all boundaries.

The results of poststack (i.e., zero-offset) depth migration of the exploding-reflector and zero-offset sections using the true velocity for the migration are shown in Figure 4, again for models M1, M2, and M4. We used an f-x domain, finite-difference depth-migration algorithm (Claerbout, 1985) for both migrations. For all models, depth migration of the exploding-reflector data yields high-quality imaging of the primaries, with artifacts related to migration of the multiples. In contrast, depth migration of the zero-offset sections results in degraded imaging of the sub-salt reflectors, especially in regions of the model where the chirp has smaller wavelength. Since these migrations were performed using the correct velocity model, the compromised migrated ZO data offer a poor starting point for study of sub-salt imaging when smoothed, erroneous velocity models are used for the migration.

Using equation (12) of Spetzler and Snieder (2004), we calculated approximate focal depths (depths at which caustics and triplications start to appear) for the six velocity models used in the study. Although only roughly approximate because that equation assumes 1D lateral slowness variations and point sources, these computed focal depths give a measure of the relative complexity of the various models and of wavefields in them. For our generic models, this complexity, which depends on the depth and lateral variation of the velocity anomaly, is controlled mainly by the geometry of the chirp. Figure 5 shows the focal depths below the surface as a function of lateral position x for the six chirp models. Model M2, for example, has caustics that appear at the shallowest depth, whereas caustics arise deeper for the models with milder chirp shape, and for chirp shape at the base rather than the top of the salt. The relatively poor image, in Figure 4, of the migrated zero-offset data for Model 2, as compared with the migrated images for models M1 and M4, suggests dependence of image quality on model complexity. (Again, the imaging problem arises because zero-offset migration is based on the exploding-reflector idea.) Also, as seen in Figure 5, the levels of complexity of models M1 and M4 are equivalent. Consistent with this observation, the image quality of the depth-migrated zero-offset sections for these models is comparable.

When errors are present in the velocity model, t he degradation of migrated ER data will differ from that in (1) poststack-migrated ZO data, (2) prestack-migrated ZO data, and (3) prestack-migrated full-offset data. Even with the correct velocity model the quality of imaging can be compromised in each of these treatments of data. We've already seen in Figure 4 that, because poststack migration is founded on the ER assumption, poststack-migrated ZO data is erroneous even when the correct velocity model is used for migration. Prestack-migrated ZO data do not suffer from that shortcoming, but can exhibit image distortion and artifacts arising from insufficient pre-migration muting of wide-angle reflections and refractions prior to the migration, limited aperture for the (shot-record) migration, and variations in wavefield illumination beneath the salt. Prestack-migrated, full-offset data can also be distorted because of variable illumination, insufficient muting, and limited migration aperture. These data, however, have the advantage that the worst of these problems are mitigated to some extent by destructive interference of offset-dependent distortions and artifacts after stacking the migrated data for all offsets.

4 LENGTH SCALES FOR VELOCITY SMOOTHING

For finite-difference migration, if we knew the velocity model perfectly we would have no need to smooth the velocities. Smoothing could only alter the model from

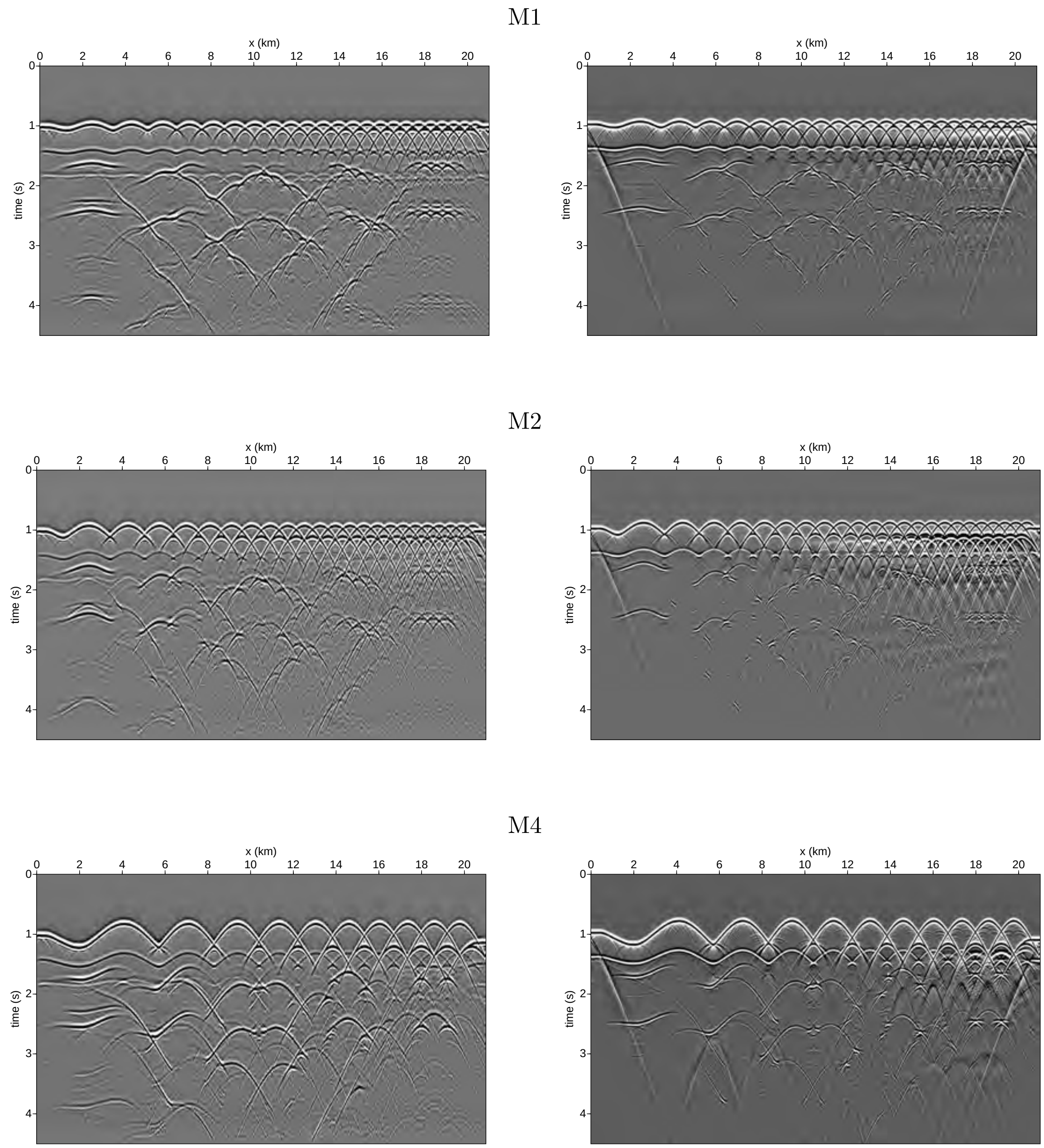

Figure 3. Exploding-reflector sections (left) and zero-offset sections (right) for models M1, M2, and M4.

the true one, resulting in erroneous migration — the more smoothing the poorer the image. Versteeg (1993), however, showed that there is little harm done with an amount of spatial smoothing that is small in relation to the wavelengths in the signal and fineness of detail in the velocity model. Even for Kirchhoff migration, Gray (2000) pointed out that smoothing too little is better than smoothing too much.

Before addressing smoothing of erroneous velocity models, let us see how much smoothing of our correct generic models is acceptable for the depth migration. Given the range of complexities suggested for the models in Figure 5, we expect that the appropriate amount of smoothing will differ from one model to another.

We smooth the velocity functions using a two-dimensional Gaussian-shaped operator similar to the

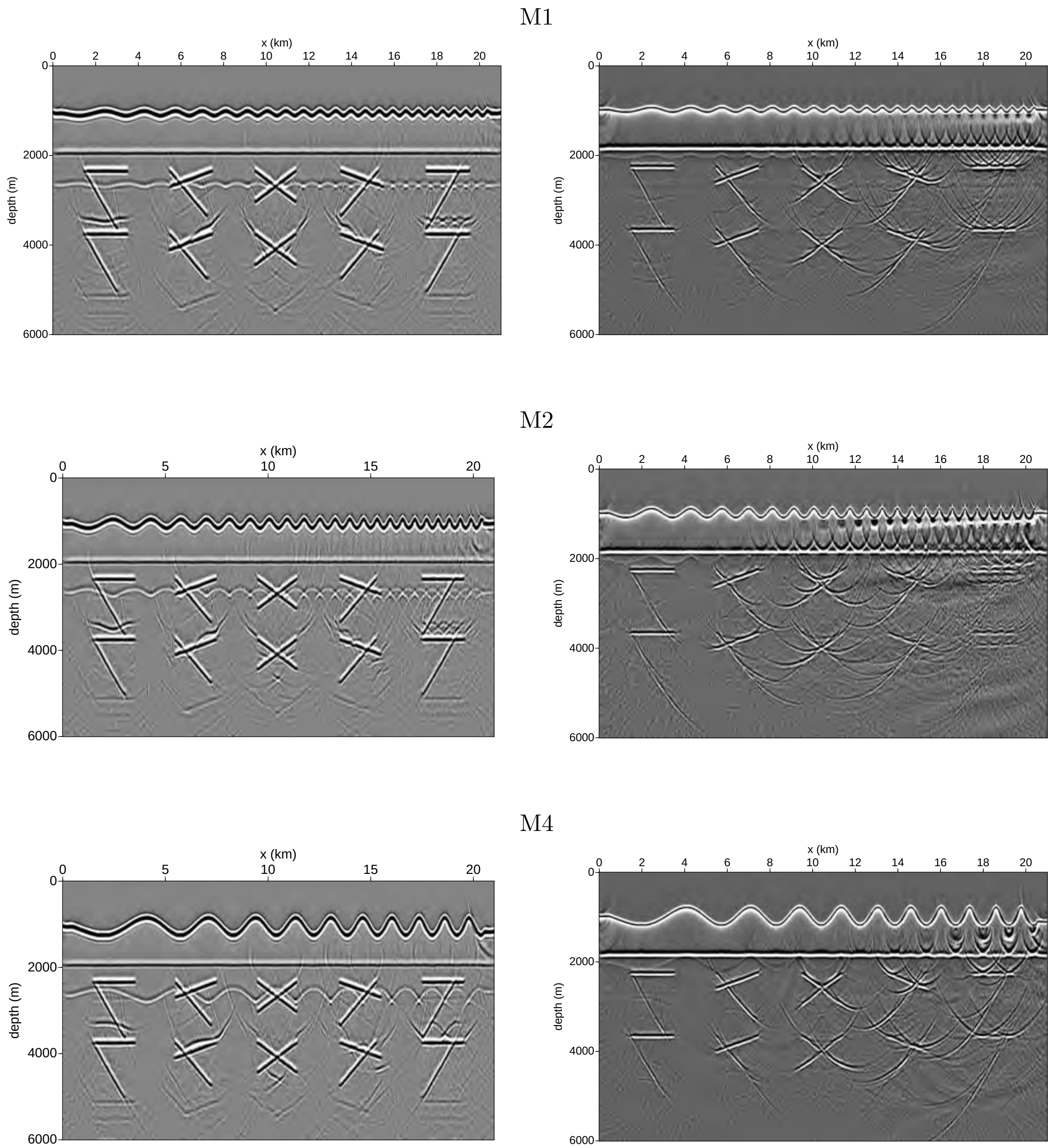

Figure 4. Finite-difference, zero-offset depth migrations of exploding-reflector data (left) and zero-offset data for models M1, M2, and M4 using the correct velocity model.

one described in Vertsteeg (1993). We first convert the velocities to slownesses and then convolve the slownesses with a two-dimensional Gaussian filter of the form $\exp[-(x^2+z^2)/(a/2)^2]$. With this definition, a is the diameter at which the amplitude of the Gaussian operator has decreased to e^{-1} of its peak value.

Although we did tests with all six models shown in Figure 1, here we focus attention primarily on models M2 and M4, the ones with the largest amplitude chirp shape for the top of salt. The conclusions drawn from tests for these two models have general counterparts from those for the other models. Figures 6 and 7 show depth-migrated exploding-reflector sections for models M2 and M4 after applying different amounts of smooth-

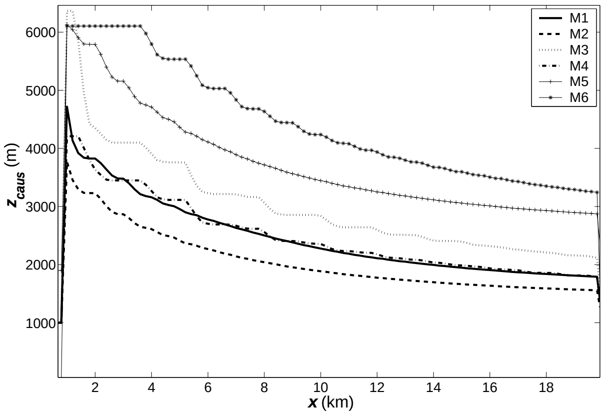

Figure 5. Focal depths z_{caus} for the velocity models in Figure 1. We associate shallower focal depth with larger model complexity.

ing to the correct velocity model. Not surprising, as the degree of smoothing increases, the quality of the imaged sub-salt reflectors worsens; for any given amount of smoothing, the degradation is model-dependent. The more complex the overburden model (i.e., the shallower the computed focal depth shown in Figure 5), the faster the image degrades with increased smoothing. Thus, for a given amount of smoothing, the degradation for model M2 is more severe than that for model M4. For both, the degradation is worse beneath the shorter-wavelength portion of the chirp. For these two models, the maximum smoothing diameter that yields acceptable imaging is about 160 m. For the remaining models, a smoothing diameter of 200 m, and even larger, yields acceptable imaging of the target reflections.

The models in which the bottom rather than the top of the salt has the chirp shape can be smoothed as much as 400 m without introducing significant distortion of the imaged sub-salt reflections. One reason for this is the closer proximity of the chirp boundary to the targets. Another is that the impedance contrast, and consequently the lateral velocity variation, is smaller for the models with chirp-shape bottom rather than top of the salt.

We note that our observations and impressions of image quality are subjective, based on assessment of four characteristics of imaged reflectors: their locations, sharpness of imaged events, distortion in imaged reflector shape, and contaminating artifacts.

As seen especially in Figure 7, the deeper targets suffer somewhat larger distortion than do the shallower ones. The farther waves have propagated through the velocity model the more complicated they become. Keep in mind that it is not the complexity of the velocity model directly above a reflector that influences the quality of imaging, but rather the complexity along the dominant ray directions. Thus the steep reflectors on the right side of the figures are better imaged than are the horizontal ones. Conversely, the horizontal reflectors at the left are better imaged than are the dipping ones there.

Another aspect of smoothing, seen in Figure 8, are gaps in the imaged bottom of the salt for model M2 migrated using velocities smoothed with a=160 m. The smoothed velocity model does not have the detail necessary to honor all the ray bending and multi-pathing that occurs at the chirp interface. As a result, migrating with the smoothed velocity model creates illumination gaps in the bottom-of-salt reflection.

To summarize, for migration with finite-differences, smoothing of the true velocity model can only degrade the imaging quality; it cannot improve it. For the generic velocity models with chirp-shape top of salt, the maximum amount of smoothing that produces an acceptably depth-migrated image is that with $a \approx 200$ m. This maximum acceptable smoothing, however, depends on the complexity of the model. In agreement with the results of Versteeg (1993) and Gray (2000), the less complex the model, the more smoothing that is acceptable. Again, however, in practice we cannot know the velocity model in detail. Next we investigate what happens when we smooth erroneous velocity models.

5 SMOOTHING OF ERRONEOUS VELOCITY MODELS: EXPLODING-REFLECTOR DATA

Here, we again consider poststack depth migration of exploding-reflector data generated for the generic velocity models. We first migrate using the erroneous velocity model and then repeat the migration after applying different amounts of smoothing to the erroneous velocity model. We introduced errors of the following kind to the generic velocity models:

- lateral and vertical shifts of the chirp-shape top or bottom salt boundary,
- erroneous amplitude of the chirp-shape boundary,
- random perturbations added to the chirp,
- erroneous velocity of the salt layer.

As simple as is our generic velocity model, the list of model parameters shown in Section 3, plus all the scale lengths (Fresnel zone, chirp wavelength, smoothing diameter, scale length of the velocity error, depth of the targets) involved in the problem make systematic analysis of depth migration for different smoothings of erroneous migration velocities a large task. We show only a few selected examples that illustrate main observations of the study.

The benefit or harm done by velocity smoothing depends on the type of error. For migration of field data in practice, velocity models will have a combination of all the forms of error that we introduce individually in this study.

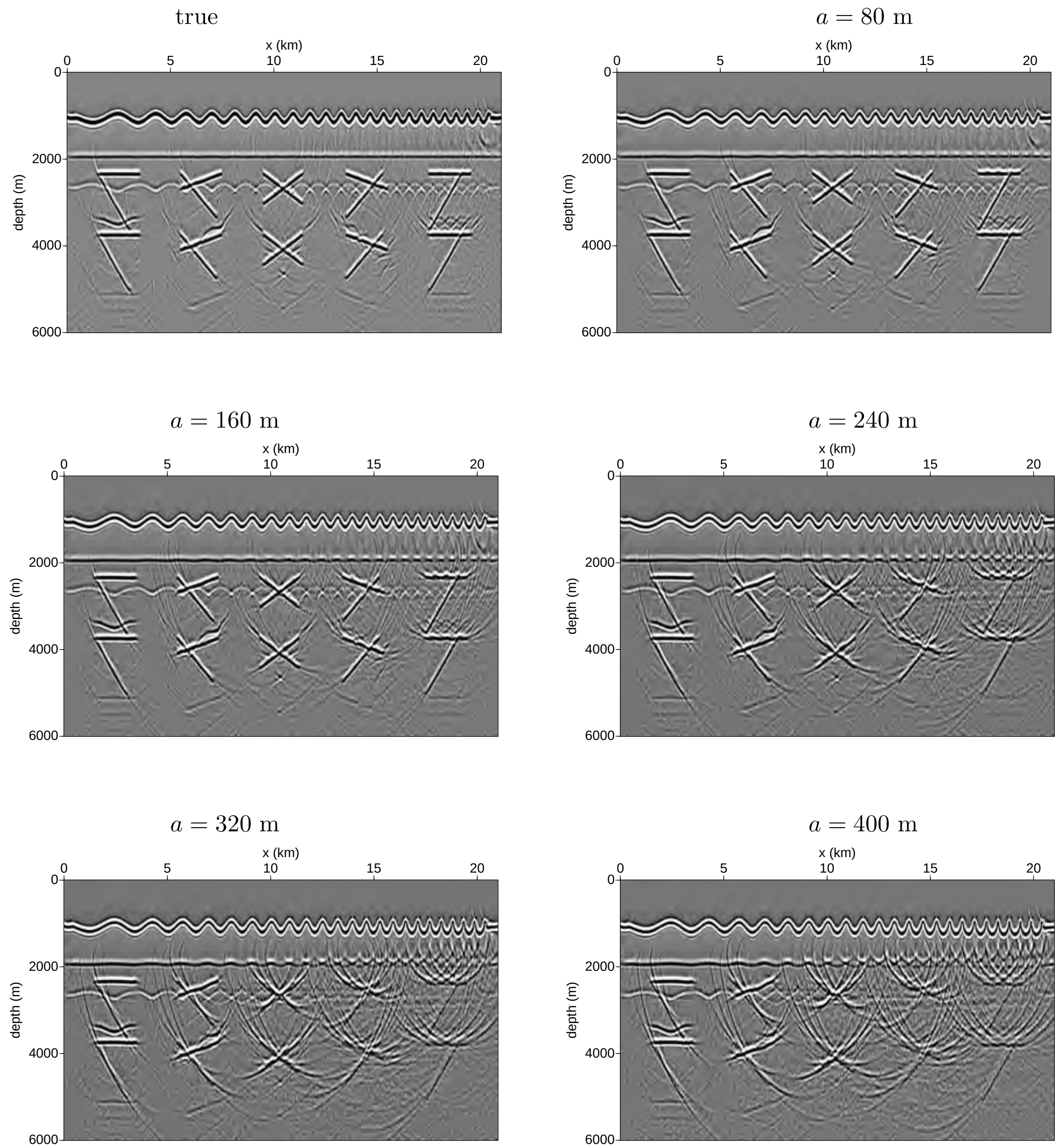

Figure 6. Depth-migrated exploding-reflector sections for model M2 using the correct velocity model and after different amounts of smoothing have been applied to that correct model. The diameter of the two-dimensional Gaussian smoothing operator is denoted by a.

Some types error in the velocity model have relatively small influence on the migrated image. For example, vertical shifts of the salt boundary and constant error in the velocity of the sediments surrounding the salt body have relatively little influence on sub-salt image quality. These two types of error primarily cause error in reflector depth without severely distorting or defocusing the image. Pon and Lines (2004) and Paffenholz et al. (2001) obtained similar results with their modeled data sets. Smoothing of these erroneous velocity models has much the same influence on the quality of imaging as does smoothing of the correct velocity models. Increasing the degree of smoothing in this case only further degrades image quality.

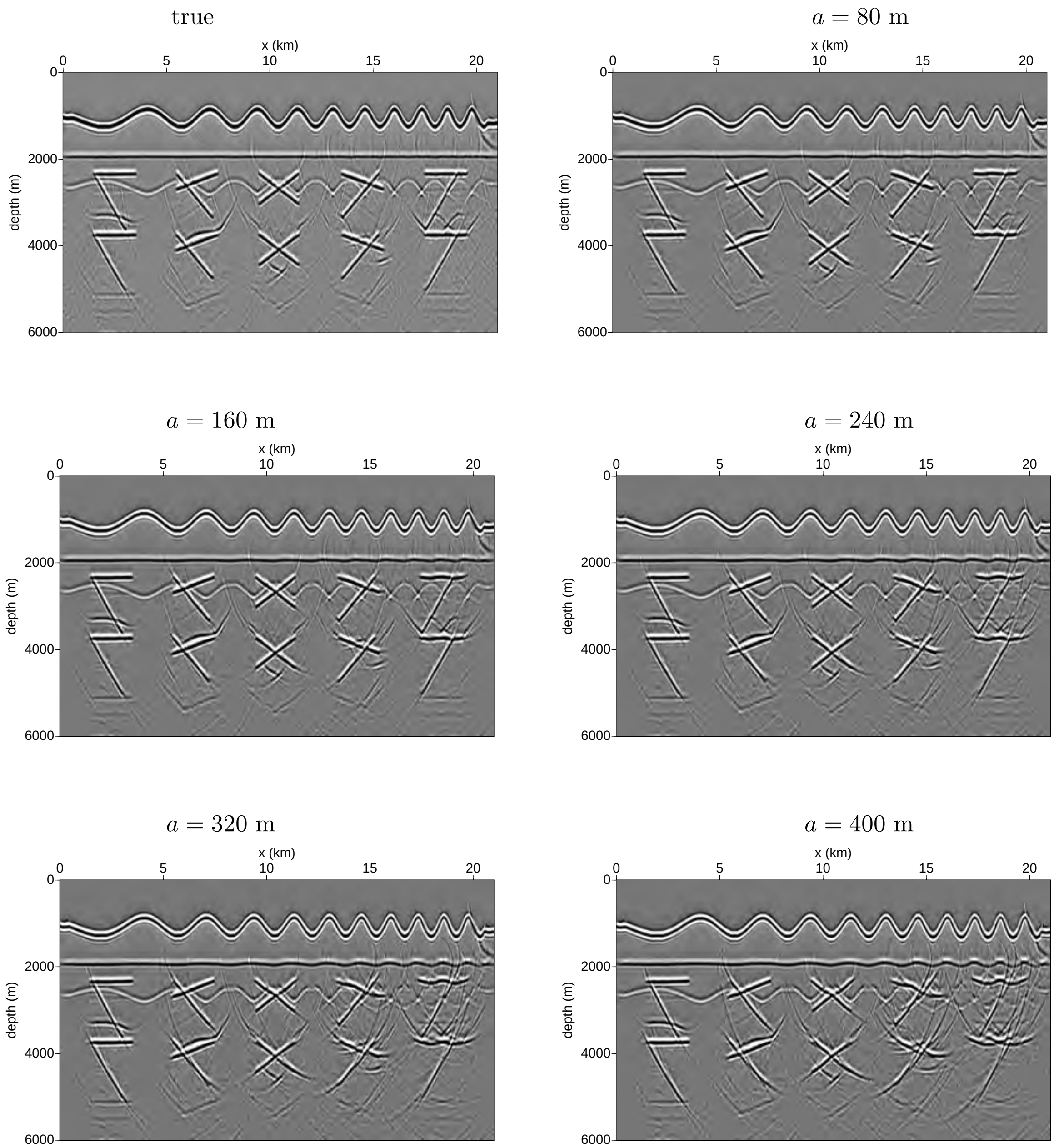

Figure 7. Same as Figure 6, but for model M4.

In contrast, consistent with the results of Paffenholz et al., we find that lateral shift of the chirp model can cause significant degradation of sub-salt imaging, as do errors in the geometry of the chirp boundary. In general, a given amount of lateral shift of the boundary causes larger degradation of the sub-salt image than does a comparable vertical shift.

As we shall see, where error in the velocity model causes substantial degradation of the migrated image. smoothing the erroneous velocity model can improve the quality of the migrated image. Where it causes too severe degradation, once again no smoothing can help.

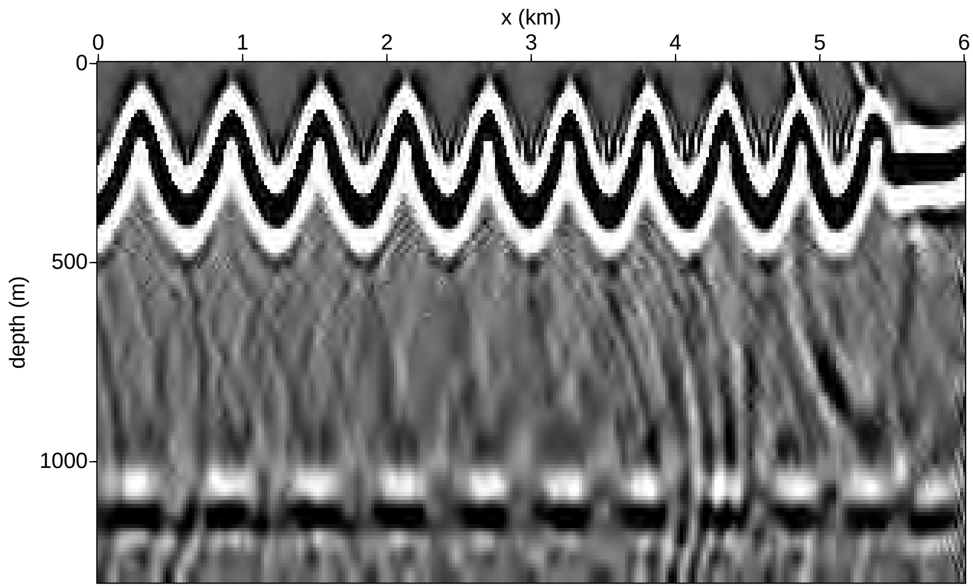

Figure 8. Close view of the top and bottom of salt in the migrated image of model M2 for velocity smoothing with a=160 m. Note the gaps in the image of the base of salt, in part the result of mistreatment of variable illumination at the salt base.

5.1 Lateral shift of the chirp

A constant lateral shift of the entire salt boundary is an unrealistic error in practice. Applied to our chirp-shape top-of-salt boundary, however, a constant shift allows us to study the influence of such an error systematically as a function of lateral velocity variation in the overburden.

Figure 9 shows the depth-migrated sections for model M4 using the correct velocity model and that model laterally shifted by different amounts, from 20 to 100 m. Note that even a shift of only 40 m (trace spacing in the exploding-reflector section is 20 m) introduces distortions in the depth-migrated image. As expected, image degradation is larger beneath the small-wavelength region of the chirp and deeper in the section. Increasing the amount of lateral shift leads to worsened image quality beneath the longer-wavelength portions of the chirp. We next smooth the shifted velocity models and assess the quality of sub-salt imaging in the resulting migrations. Figure 10 shows migrations with smoothed versions of the model that was erroneously shifted laterally by 40 m. Smoothing with a of 160 to 240 m improves the image quality for many of the sub-salt targets, but smoothing by larger amounts results in reduced quality of the migrated section. Smoothing of velocity models with larger lateral shifts (not shown here) produced similar results although the improvement introduced by smoothing becomes harder to recognize for larger shifts. The data quality is so much compromised for large lateral shift that smoothing can have little influence. The image quality is already so poor that it would take a large amount of smoothing to make it much worse.

5.2 Exaggerated chirp amplitude

The type of velocity error we consider next is that caused by incorrect amplitude of the chirp-shape top of salt. Figures 11 and 12 show depth-migrated images of exploding-reflector data for models M2 and M4, each with the amplitude of the chirp-shape top of salt too large by 50 m, and with various amounts of smoothing. The images for the erroneous models are significantly degraded from those generated with the correct migration velocity, more so for model M2 (with short spatial wavelength of chirp) than for model M4. Smoothing of the erroneous velocities for model M2 results in improved image quality for smoothing diameter up to about 320 m, but degrades the quality for larger smoothing. The degree of improvement varies across the model. For model M4, improvement in imaging for some targets is best with a as large as 640 m. Note also that the region of largest improvement generally progresses toward the left (i.e., toward longer spatial wavelength of chirp) as the amount of smoothing increases.

For this 50-m error in chirp amplitude, we performed migrations of models M1 through M4 (the four models with chirp-shape top of salt) and smoothing ranging from a = 80 m to 1240 m in increments of 40 m. From subjective visual impressions of migrated sec-

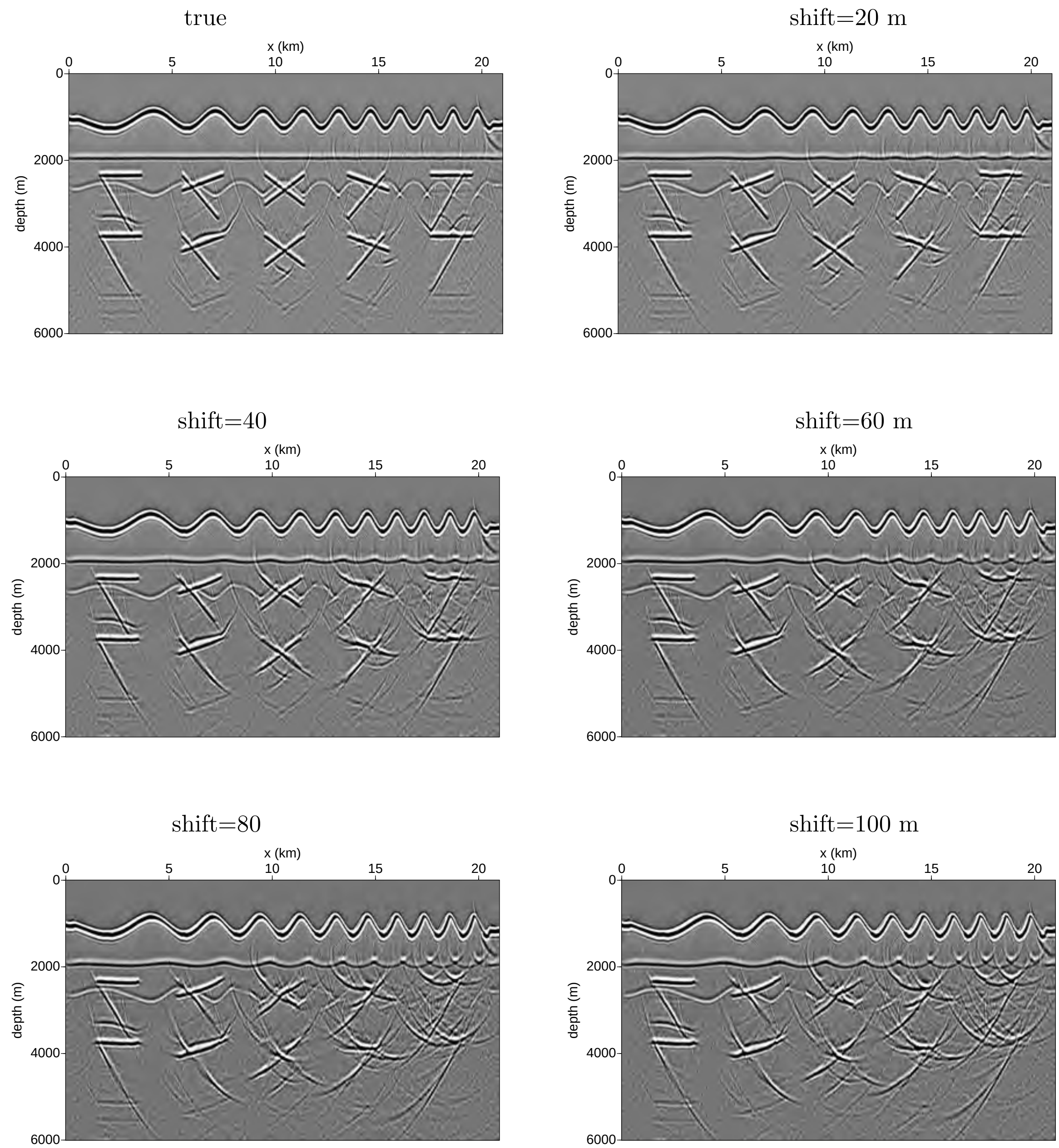

Figure 9. Depth-migrated exploding-reflector sections for model M4 using the correct velocity and different amounts of lateral shift of that model.

tions for the different amounts of smoothing, we made rough estimates of smoothing diameter that yields the best imaging of the different target reflectors across the model. Figure 13 shows the estimated optimum smoothing diameters for the four models, as a function of lateral position x. Comparison of the curves (linearly interpolated between the subjectively inferred values) in this figure with the curves in Figure 5 shows some degree of correlation between the focal depths in Figure 5 (a measure of model complexity) and the optimum smoothing diameters in Figure 13 for this particular form of velocity error: generally the shallower the focal depth (i.e., the greater the model complexity), the smaller the smoothing diameter that is best.

Versteeg (1993) showed that the lower the complexity of the velocity field, the larger the amount of smooth-

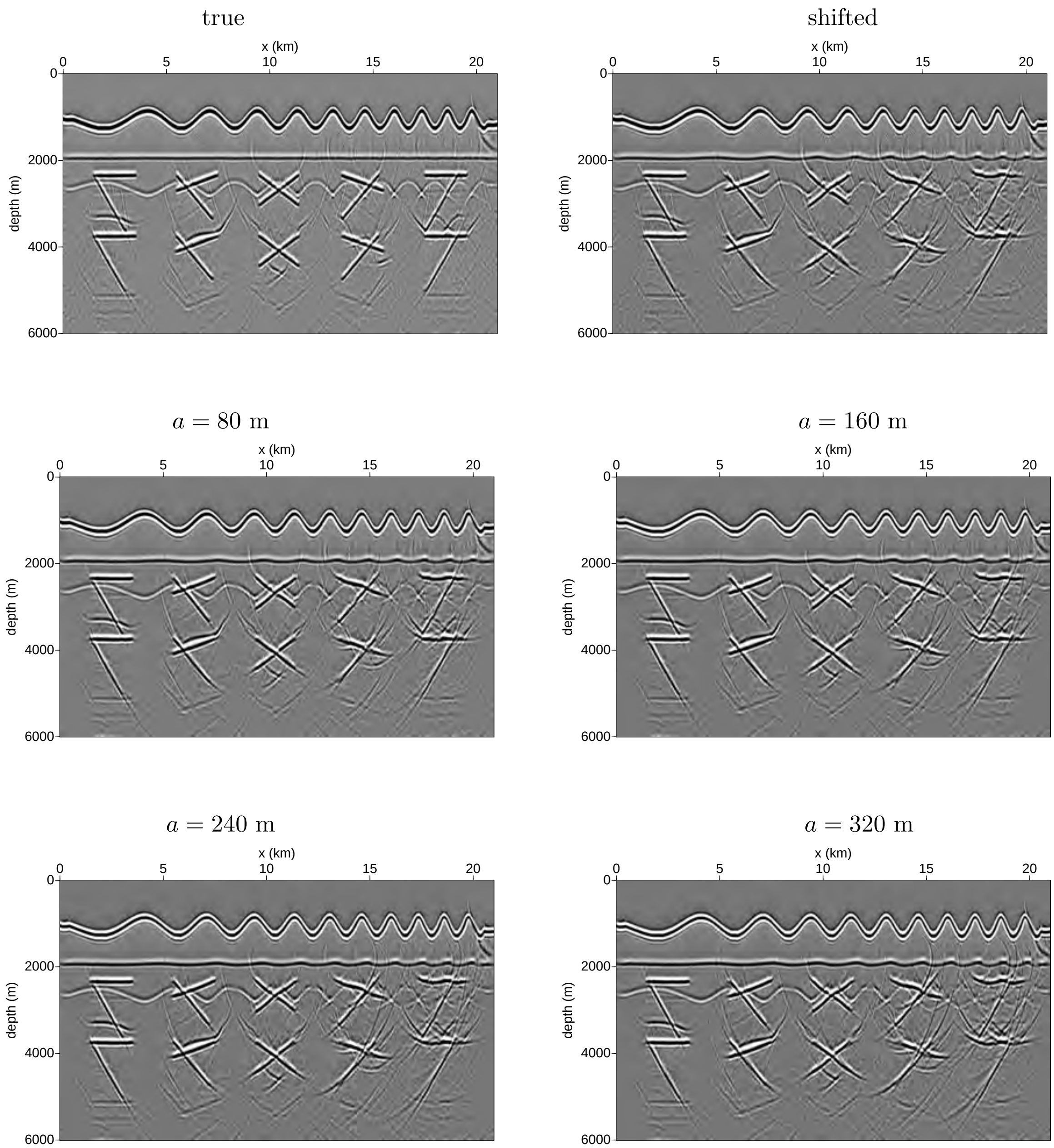

Figure 10. Depth-migrated exploding-reflector sections for model M4 using the correct velocity model, for that model laterally shifted by 40 m, and for various degrees of smoothing applied to the laterally shifted model.

ing of the velocity model that is acceptable for imaging. Here, we find a counterpart result: the lower the complexity of the velocity field, the larger the amount of smoothing that yields the best imaging when the initial model is in error. In tests with larger error in chirp amplitude (100-m too large), we found a similar correlation between model complexity and optimum amount of smoothing.

5.3 Random perturbation of the chirp

The final type of error in the migration-velocity model that we show is a random perturbation of the chirp-

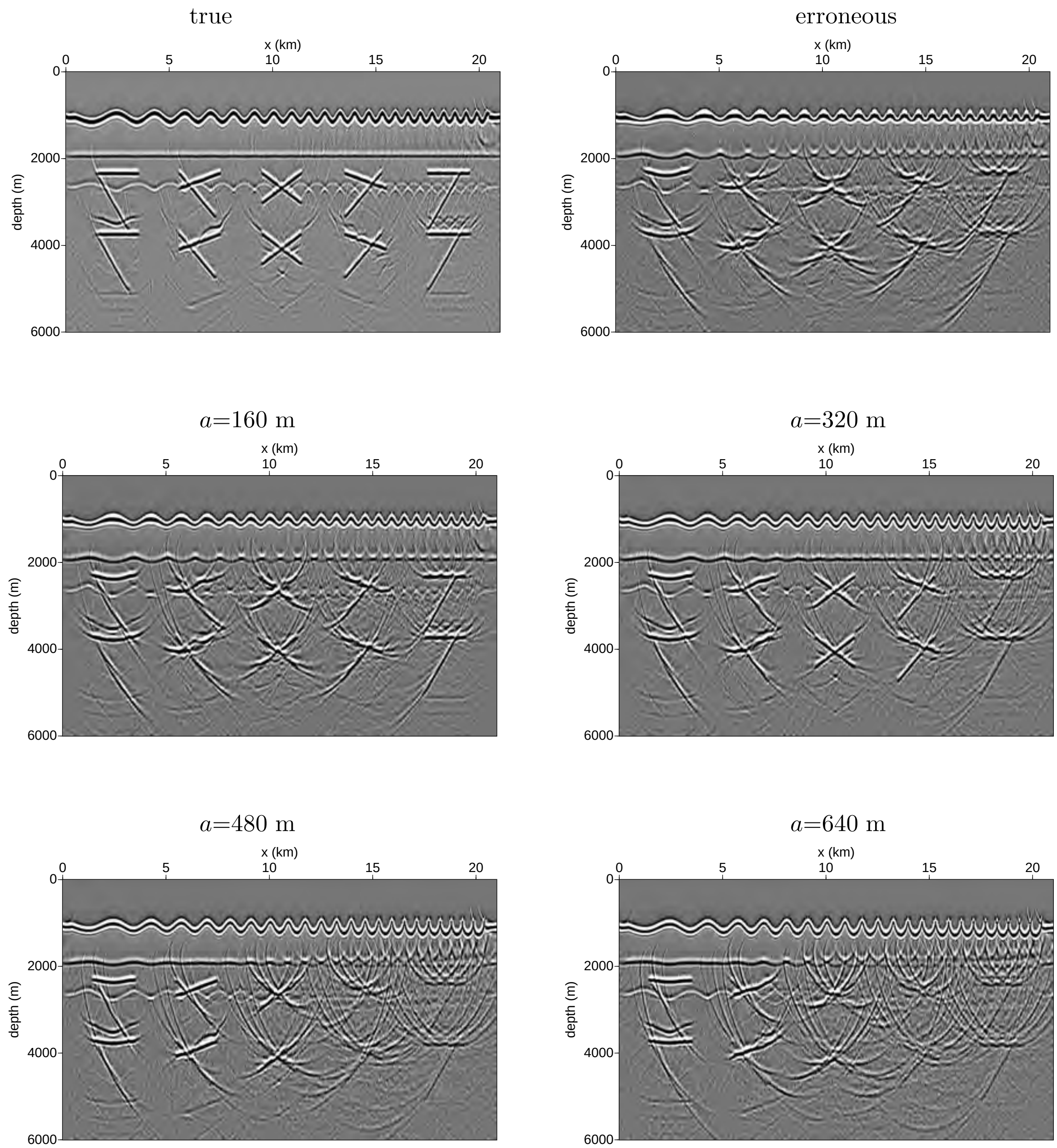

Figure 11. Depth-migrated exploding-reflector sections for model M2 with true velocity, for an erroneous velocity model caused by chirp amplitude exaggerated by 50 m (a 50 percent exaggeration), and for smoothed versions of the erroneous velocity model.

shape top of the salt. We distorted the shape by adding a laterally bandlimited, Gaussian-distributed depth error to the chirp. For the test results shown in Figures 14, 15, and 16, the correlation length $l = 100$ m, where l is the lag at which the autocorrelation of the random depth variation decreases by a factor e^{-1} of its peak value. The correlation length is a measure of lateral scale length of velocity error. For these tests, the standard deviation of the random depths prior to bandlimiting is $\sigma = 50$ m.

Figures 14 and 15 show migrated sections using the true velocity model, a model with random error added to the depth of the chirp, and variously smoothed versions of the erroneous velocity function for models M2 and M4. For both models, migration with the erro-

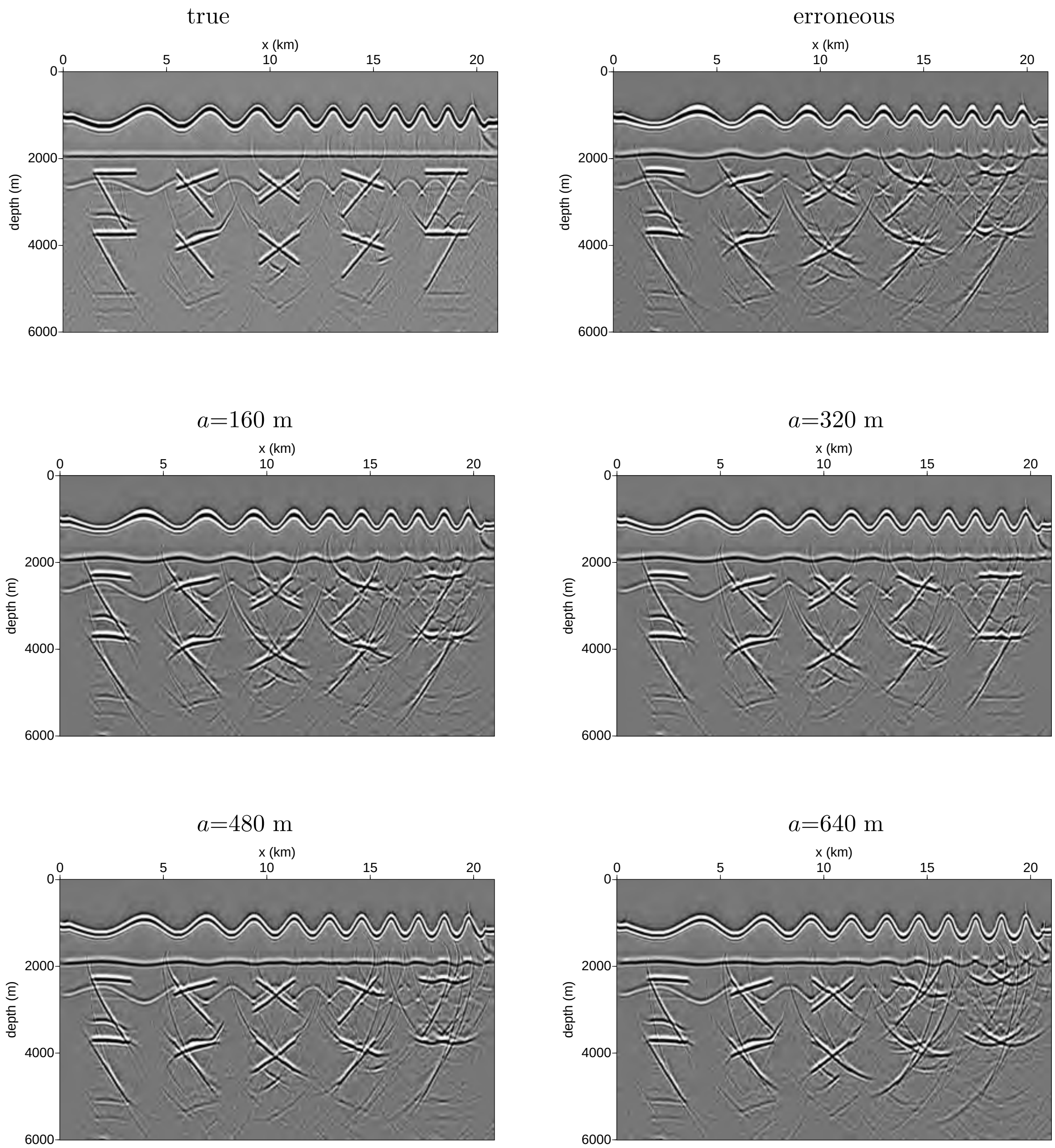

Figure 12. Same as Figure 11 but for model M4. The 50-m increase in chirp amplitude represents a 25 percent exaggeration of the amplitude for this model.

neous velocity function yields severely distorted imaging of the sub-salt reflections. For model M2 (Figure 14), which has the shorter-wavelength chirp-shape top of salt, smoothing of the erroneous velocity model yields, at best, marginal improvement, with optimal smoothing varying from $a = 160$ m to at least 640 m for reflectors from right to left. The improvement brought about by smoothing the erroneous model is more evident in the results for model M4, shown in Figure 15. As smoothing increases from $a = 160$ m to 640 m, targets that are best imaged again are those beneath progressively longer-wavelength portions of the chirp.

Model M3 has chirp shape spanning the same range of wavelengths as those in model M4, but with smaller-amplitude chirp. Compared to results for similarly considered models M2 and M4, migration for data from

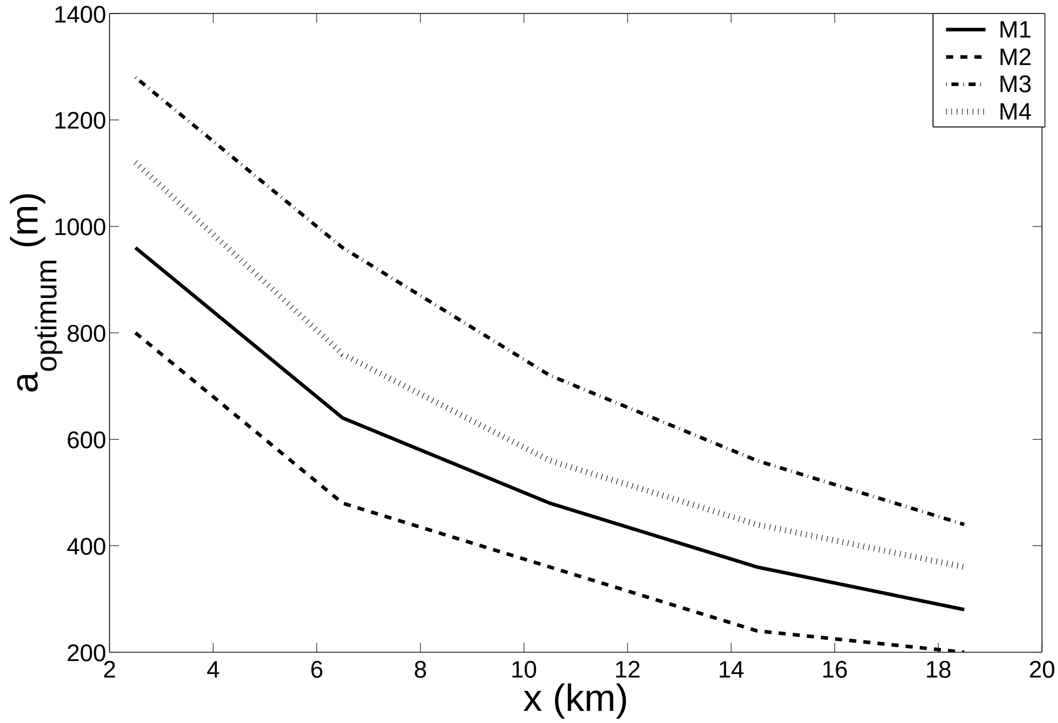

Figure 13. Optimum smoothing diameters for migration-velocity error caused by chirp amplitude that is 50-m too large, for models M1-M4.

model M3 (Figure 16) exhibits more distortion of sub-salt events when the randomly erroneous velocity model is used. Migration with variously smoothed versions of the erroneous model, however, yields substantial improvement in sub-salt images. The pattern of improved quality of imaging for various smoothings of the erroneous velocity model is similar to that seen in Figures 14 and 15, but the improvement here is dramatic. In particular, much of the sub-salt region is best imaged with smoothing using $a = 320$ and 640 m, with $a = 640$ m yielding the best result for lateral positions $x < 10$ km. Even broader smoothing might have resulted in a better image yet. We found similar behavior for other choices of correlation distance and amplitude of the random perturbations. Smoothing of the migration-velocity model *can* help in imaging.

6 SMOOTHING OF AN ERRONEOUS VELOCITY MODEL: PRESTACK MIGRATION

In all of the above tests, we have used poststack-migrated exploding-reflector data to assess the influence of smoothing of erroneous velocity models on sub-salt image quality. Such data and migration require so relatively little computation that we could perform a large number of tests. Despite being useful for our study, exploding-reflector data cannot be acquired in the field nor can they be obtained from field data. They are a fiction. Next we show results for one example of a similar study of the influence of smoothing, but with prestack migration performed on synthetic multi-offset data.

Using finite-difference code, we modeled shot records for a simulated 2D survey across the top of model M4, each shot having 500 channels, with 10-m group interval, and 80-m shot spacing. Migration was performed with a shot-record f-x domain algorithm (Claerbout, 1985). We then sorted the migrated data into common-image gathers and stacked the gathers. Figure 17 shows the prestack-migrated image for model M4 using the correct velocity model. The quality of imaging for the target reflectors is excellent, superior to that obtained in poststack migration of exploding-reflector data for model M4 (Figure 4), primarily because imaged multiples are much weaker in the prestack result.

For this test, we generated the erroneous velocity model by exaggerating the amplitude of the top-of-salt chirp in model M4 by 100 m, a 50 percent increase from the true chirp amplitude. Prestack migration with this erroneous velocity model is shown in the upper left of Figure 18. With this level of velocity error, the shape of the horizontal bottom of the salt is greatly distorted toward the left of the section, and toward the right the bottom of the salt is virtually not imaged. Similar obser-

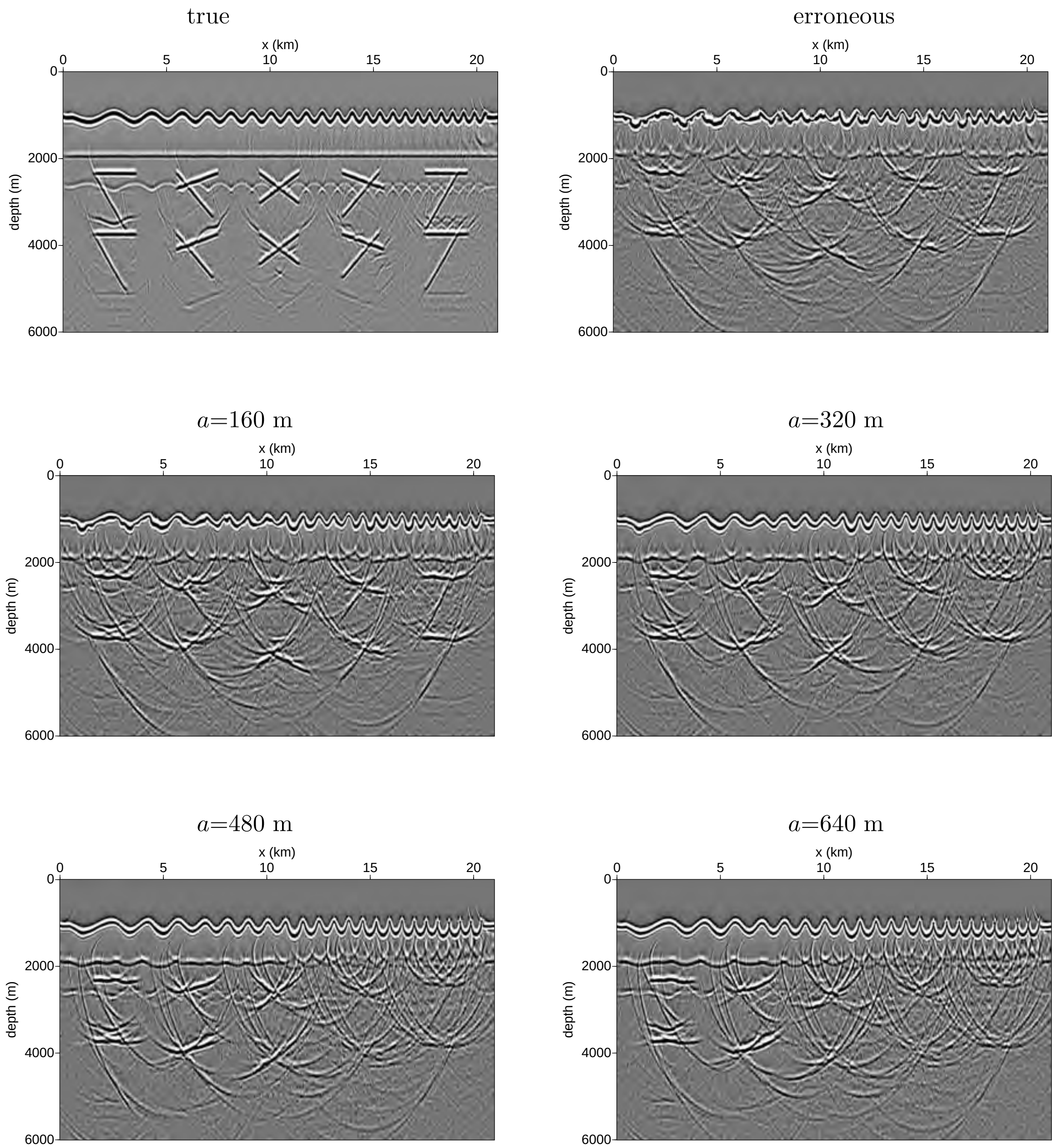

Figure 14. Depth-migrated exploding-reflector sections for model M2 with the true velocity, for an erroneous velocity model with random error ($l = 100$ m, $\sigma = 50$ m), and for variously smoothed versions of the erroneous velocity model.

vations hold for the sub-salt reflectors. The remainder of the figure shows the results of prestack migration using the erroneous velocity model smoothed with what we might consider to be large amounts of smoothing: $a = 240$, 480, and 720 m. Velocity smoothing clearly improves the quality of the migrated images, with $a = 480$ m yielding the best imaging of the right portion of the subs-salt section (beneath the shorter-wavelength portion of the chirp), and $a = 720$ m yielding the best imaging beneath the longer-wavelength portion. The best images show distortion of the shapes of the target reflectors, but these reflectors nevertheless are far better imaged than when no smoothing is applied to the erroneous velocity model.

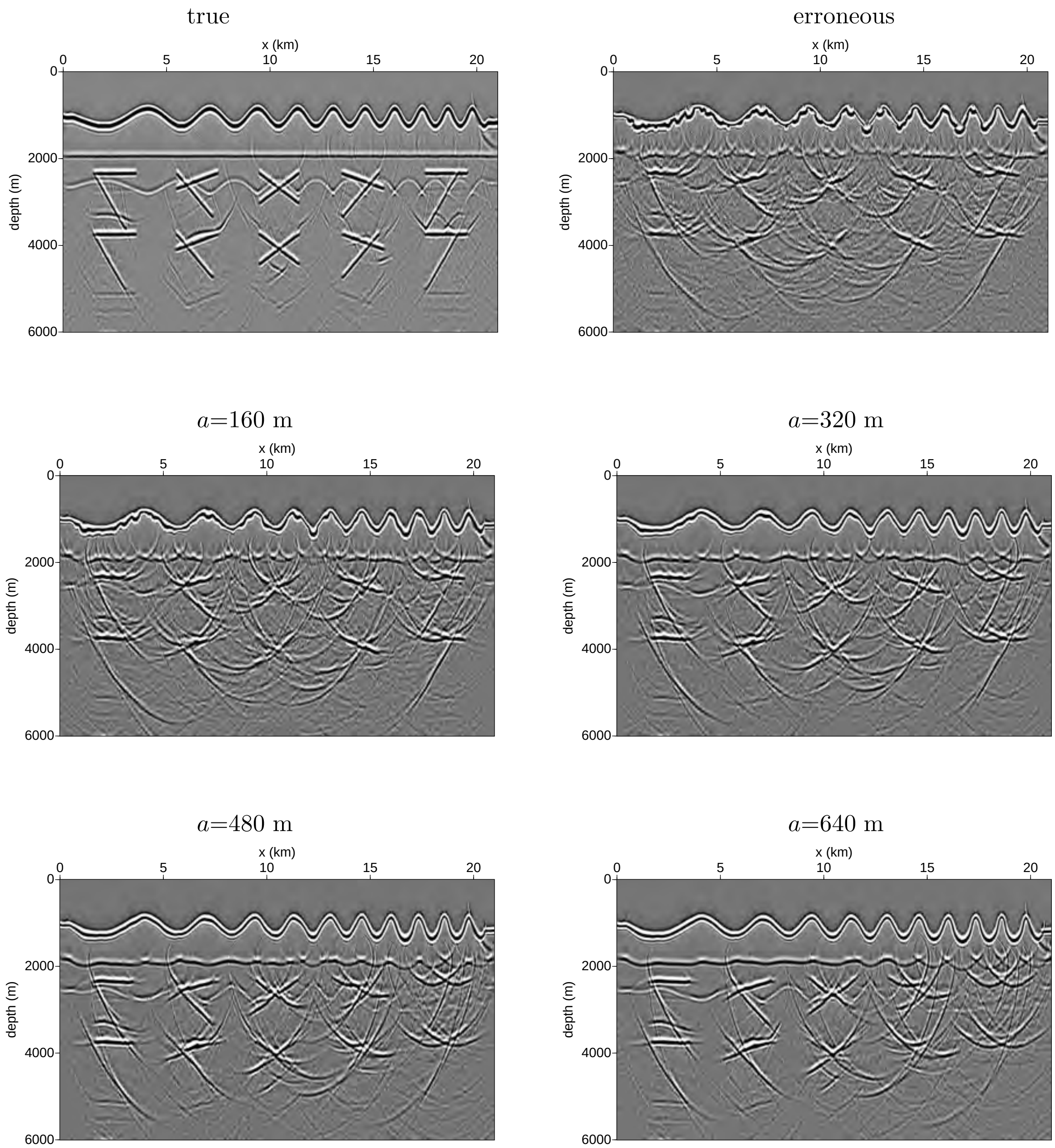

Figure 15. Same as Figure 14 but for model M4.

Prestack migration with the erroneous velocity model resulted in more severe degradation of image quality than did poststack migration of the exploding-reflector data. This could be due in part to mistacking that arises when the incorrect velocity model is used. In any case, the data are far better imaged with use of smoothed migration velocities in the migration.

7 DISCUSSION AND CONCLUSIONS

Despite the limited nature of this study — 2D, primarily poststack migration of exploding-reflector data, just one choice of wavelet, simple chirp-shape top or bottom of salt with limited range and choice of spatial wavelength, small number of and forms for perturbations from the true velocity model, and simple model of subsurface structure — results for tests with the generic

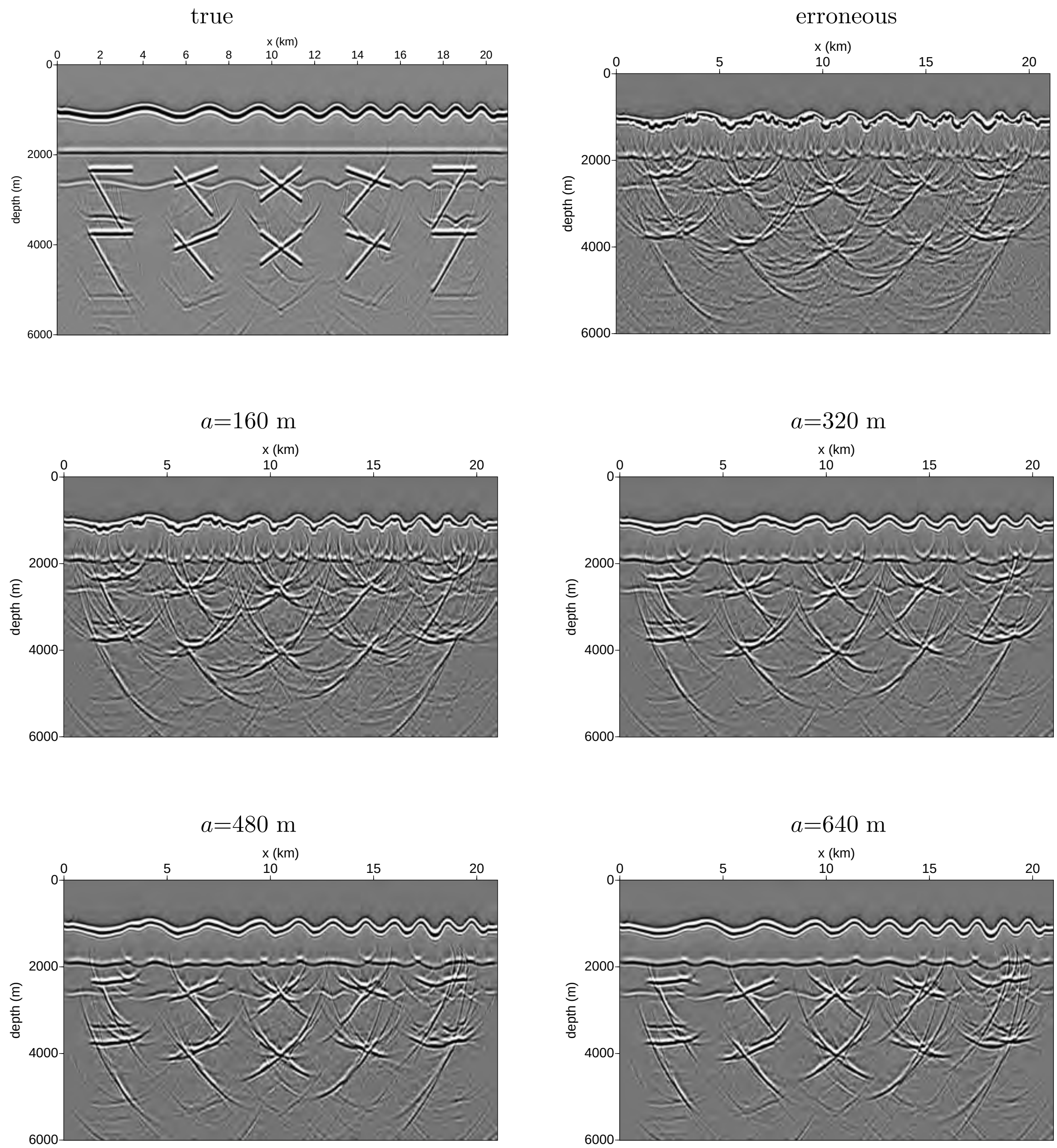

Figure 16. Same as Figure 14 but for model M3.

model give clear indication that, for some types of velocity error, smoothing of velocities for migration velocity model *can* improve image quality, sometimes significantly. The amount of smoothing that is optimum in the sense that it gives imaging superior to that when either less or more smoothing is used depends on the size and type of error in the migration-velocity model as well as on the lateral wavelength of the true velocity structure in the overburden.

The optimal choice for smoothing to address imaging degradation caused by use of an erroneous velocity model can be considerably larger than either (1) that needed to overcome shortcomings of ray tracing for Kirchhoff migration or (2) the amount of smoothing that would be acceptable for any migration algorithm

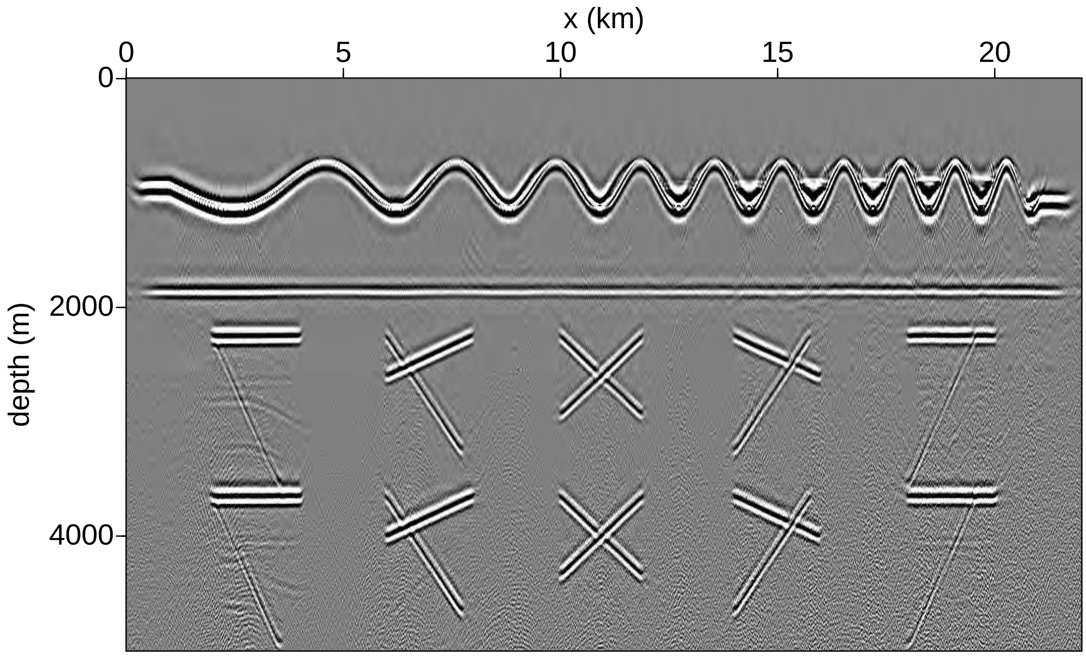

Figure 17. Prestack migrated image for model M4 using the correct velocity model. Compare with Figure 4.

when the initial migration-velocity model was perfectly accurate. Because the velocity function for migration is never fully accurate in practice, *some* degree of smoothing is always appropriate. Moreover, although it will be difficult in practice to pin down an optimal spatial extent of smoothing, that amount can well be larger than is often used in practice — even considerably larger than the spatial size of the errors in the migration-velocity model.

Use of the generic chirp-shape salt boundary allowed us to do simple tests, e.g., velocity error modeled as lateral shift of the boundary, in a systematic effort to gain an idea of the relationship between optimum amount of smoothing and scale of the velocity variations. For even this simple model, we have seen dramatic differences between zero-offset data modeled based on the exploding-reflector assumption and those modeled with wavefields generated by individuals shots. A significant manifestation of the difference arises from variations in the spatial distribution of subsurface illumination. These differences in the two forms of modeled data in turn give rise to marked difference in image quality when the data are depth-migrated with a poststack algorithm (which is based on the exploding-reflector) using a migration-velocity function that is known perfectly.

Although we did only a few tests of smoothing erroneous velocity models for use in prestack migration, use of smoothed velocities generally helped to improve the quality of images — greatly so for the one test with prestack migration shown here. This is consistent with what we found (although to a lesser extent) for poststack migration of exploding-reflector data. The consistency is comforting given that most of our tests were with exploding-reflector data, which cannot be obtained from field data. Supporting the results from the poststack migrations of exploding-reflector data, the amount of smoothing that is best can be considerably larger than might have been suspected from the spatial size of errors and detail in the velocity model.

A general ranking of the influence of the different types of velocity error on image quality is as follows. Constant vertical shift of the top of salt or constant error in velocity of the overburden causes relatively little degradation. Smoothing of the velocity model will not improve imaging for these types of error any more than it would if the velocity model were perfectly accurate. Lateral shift of the top of salt causes image distortion that can be not only large, but such that imaging is not amenable to improvement by velocity smoothing. Error in amplitude of the chirp-shape top of salt, including random perturbation of the salt shape, can also cause large distortions in the sub-salt image, but the imaging can be substantially improved through use of smoothed

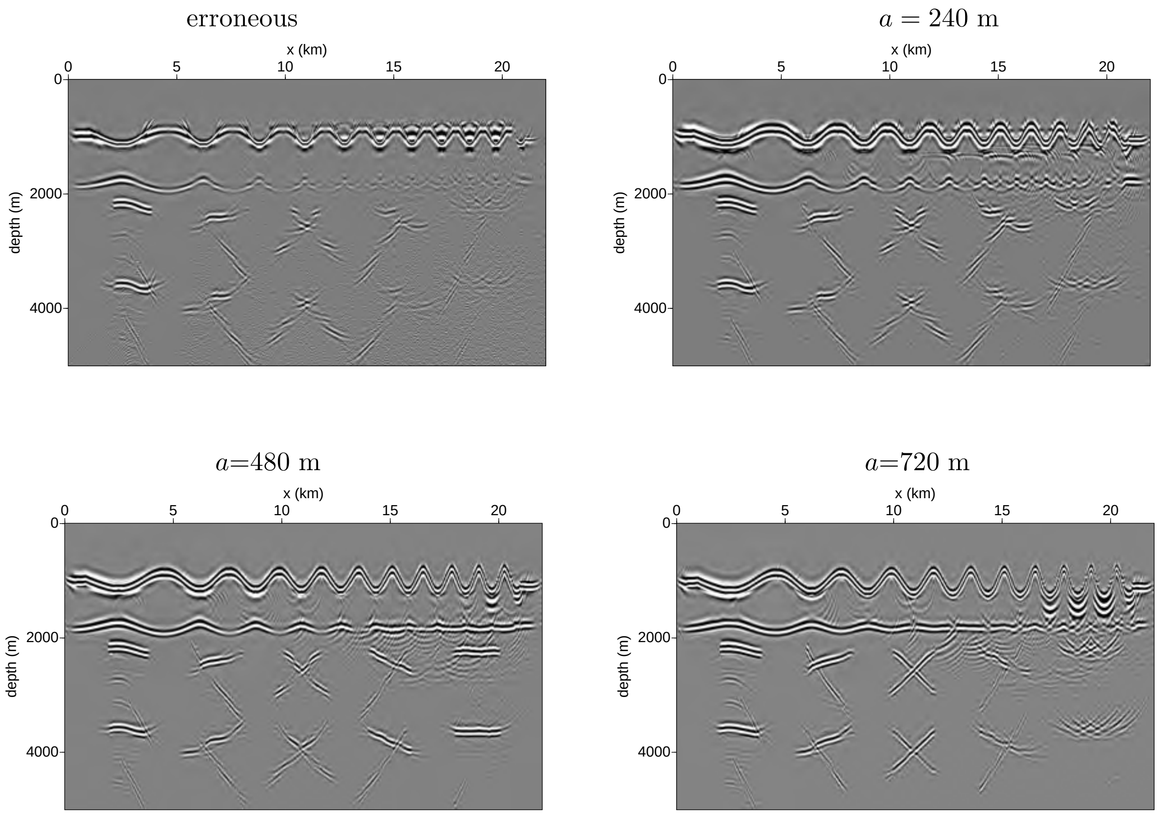

Figure 18. Prestack-migrated image for model M4 using the erroneous velocity model with chirp amplitude exaggerated by 100 m, and for the erroneous velocity model smoothed with operator diameter a=240, 480, and 720 m.

velocities, even broadly smoothed. Of course these general comments about the influences of the different types of error and the benefits of smoothing for these types of error are all dependent on the magnitude of the velocity error of any given type.

Any smoothing of a derived migration-velocity model yields velocities that are erroneous. That's clearly true if the derived velocities somehow happened to be perfectly accurate. A conclusion from the tests here is that, since the migration-velocity model is necessarily inaccurate, it is better that detail in the initial velocity model be smoothed prior to migration — thus yielding a smoothly erroneous model — than to trust in use of the detailed model. Moreover, the amount of smoothing needed to help the imaging is likely greater than that inferred from previous studies involving smoothing of perfectly accurate velocities. The observation of Gray (2000) nevertheless still holds that too much smoothing will alter the velocity model from the 'true' one to the extent that image quality will be harmed. The optimal amount of smoothing to use remains as difficult model- and data-dependent choice.

REFERENCES

Claerbout, J. 1985. *Imaging the Earth's Interior*. Blackwell.

Clayton, R., & Engquist, B. 1977. Absorbing boundary conditions for acoustic and elastic wave equations. *Bull. Seis. Soc. Am.*, **67**, 1529–1540.

Gray, S. 2000. Velocity smoothing for depth migration: how much is too much? Calgary, Alberta, Canada: CSEG Publication.

Jannane, M. et. al. 1989. Short note: Wavelengths of earth structures that can be resolved from seismic reflection data. *Geophysics*, **54**(7), 906–910.

Kjartasson, E., & Rocca, F. 1979. The exploding reflector model and laterally variable media. *In: Stanford Exploration Project No. 16*. Stanford University.

Paffenholz, J. 2001. Sigsbee2 synthetic subsalt dataset: image quality as function of migration algorithm and velocity model error. San Antonio, Texas, USA: 71st SEG Annual International Meeting.

Pon, S., & Lines, L.R. 2004. Sensitivity analysis of seismic depth migrations: Canadian Structural Model. Calgary, Alberta, Canada: CSEG Publication.

Spetzler, J., & Snieder, R. 2001. The formation of caustics in two- and three-dimensional media. *Geophys. J. Int*, **144**, 175–182.

Spetzler, J., & Snieder, R. 2004. Tutorial: The Fresnel volume and transmitted waves. *Geophysics*, **69**(3), 653–663.

Versteeg, R. J. 1993. Sensitivity of prestack depth migration to the velocity model. *Geophysics*, **58**(6), 873–882.